0026-895X/06/6905-1641–1651$20.00
MOLECULAR PHARMACOLOGY
Copyright © 2006 The American Society for Pharmacology and Experimental Therapeutics
Mol Pharmacol 69:1641–1651, 2006

Vol. 69, No. 5
20883/3103503
Printed in U.S.A.

Identification of Various Allosteric Interaction Sites on M_1 Muscarinic Receptor Using ^{125}I-Met35-Oxidized Muscarinic Toxin 7

Carole Fruchart-Gaillard, Gilles Mourier, Catherine Marquer, André Ménez, and Denis Servent

Commissariat à l'Energie Atomique, Département d'Ingénierie et d'Etude des Protéines, Gif-sur-Yvette, France

Received November 16, 2005; accepted January 24, 2006

ABSTRACT

Monoiodinated, Met35-oxidized muscarinic toxin 7 (MT7ox) was synthesized, and its affinity constants for free or *N*-methyl scopolamine (NMS)-occupied hM_1 receptor were measured directly by equilibrium and kinetic binding experiments. Identical values were obtained with the two types of assay methods, 14 pM and 0.9 nM in free or NMS-liganded receptor states, respectively, highlighting a strong negative cooperativity between this allosteric toxin and NMS. Identical results were obtained with indirect binding experiments with [^{3}H]NMS using the ternary complex model, clearly demonstrating the reciprocal nature of this cooperativity. Furthermore, the effects of various orthosteric and allosteric agents on the dissociation kinetic of ^{125}I-MT7ox were measured and show that, except for the MT1 toxin, all of the ligands studied [NMS, atropine, gallamine, brucine, tacrine, staurosporine, and (9*S*,10*S*,12*R*)-2,3,9,10,11-hexahydro-10-hydroxy-9-methyl-1-oxo-9,12-epoxy-1*H*-diindolo[1,2,3-*fg*:3′,2′,1′-*kl*]pyrrolo[3,4-*i*][1,6]benzodiazocine-10-carboxylic acid hexyl ester (KT5720)] interact allosterically with muscarinic toxin 7. Equilibrium binding experiments with ^{125}I-MT7ox and [^{3}H]NMS were conducted to reveal the effects of these ligands on the free receptor, and affinity constants (pK_x values) were calculated using the allosteric ternary complex model. Our results suggest that MT7 toxin interacts with hM_1 receptor at a specific allosteric site, which may partially overlap those identified previously for "classic" or "atypical" allosteric agents and highlight the potential of this new allosteric tracer in studying allosterism at muscarinic receptors.

An increasing body of evidence now shows that many G-protein-coupled receptors are susceptible to allosteric modulation (Christopoulos and Kenakin, 2002), and this phenomenon is particularly well documented for the five muscarinic acetylcholine receptor subtypes (Tucek and Proska, 1995; Birdsall et al., 1997; Ellis, 1997; Lazareno et al., 2004; Birdsall and Lazareno, 2005). These receptors are characterized by at least two distinct binding sites. Agonists and competitive antagonists bind to the orthosteric site, located inside the transmembrane domain, whereas allosteric agents induce a positive or a negative alteration of the orthosteric ligand affinity by interacting with an allosteric site, located more extracellularly (Stockton et al., 1983; Ellis et al., 1993; Ellis, 1997; Trankle and Mohr, 1997; Christopoulos et al., 1998; Christopoulos and Kenakin, 2002). Furthermore, recent publications report the presence of at least two distinct allosteric sites on muscarinic receptors selective for distinct classes of allosteric agents, suggesting that it is possible for three small ligands to bind simultaneously to a muscarinic receptor (Birdsall et al., 2001; Lazareno et al., 2002). For instance, staurosporine and other indolocarbazole compounds have been shown to interact at a second allosteric site on hM_1 receptor, associated with a positive cooperativity with ACh (Lazareno et al., 2000).

The effects of allosteric ligands are consistent with a ternary complex model in which the orthosteric and allosteric agents bind simultaneously to the receptor and modify each other's affinities (Stockton et al., 1983; Ehlert, 1988; Lazareno and Birdsall, 1995). Therefore, the binding and actions of an allosteric ligand with various receptors and orthosteric compounds are defined by two independent parameters, af-

Article, publication date, and citation information can be found at http://molpharm.aspetjournals.org.
doi:10.1124/mol.105.020883.

ABBREVIATIONS: ACh, acetylcholine; MT7, muscarinic toxin 7; MT7ox, Met35-oxidized muscarinic toxin 7; MT1, muscarinic toxin 1, NMS, *N*-methyl scopolamine; TFA, trifluoroacetic acid; PBS, phosphate-buffered saline; CHO, Chinese hamster ovary; HPLC, high-performance liquid chromatography; RT, retention time; W84, hexamethylene-bis-[dimethyl-(3-phthalimidopropyl)ammonium]dibromide; KT5720, (9*S*,10*S*,12*R*)-2,3,9,10,11-hexahydro-10-hydroxy-9-methyl-1-oxo-9,12-epoxy-1*H*-diindolo[1,2,3-*fg*:3′,2′,1′-*kl*]pyrrolo[3,4-*i*][1,6]benzodiazocine-10-carboxylic acid hexyl ester.

finity and cooperativity, which can generate receptor selectivity, which is useful in the context of therapeutic agents (May and Christopoulos, 2003).

Until now, except for the recently synthesized [^{3}H]dimethyl-W84 used to measure directly the affinities of various allosteric ligands for the M_2 muscarinic receptor (Trankle et al., 1998, 1999, 2003), all pharmacological characterizations of allosteric agents interacting with muscarinic receptors were derived from their indirect effects on the binding of orthosteric ligand such as NMS. Thus, the lack of radiolabeled allosteric ligands selective for the different muscarinic receptor subtypes prevents direct investigation of the interaction of allosteric agents with their specific binding sites.

For instance, approximately 10 different muscarinic toxins have been isolated from the venom of African mambas and, despite a high sequence homology, they exhibit clear differences in their functional activities and possess various profiles of interaction with the five muscarinic receptor subtypes (Bradley, 2000; Karlsson et al., 2000; Onali et al., 2005). Among these toxins, MT7 toxin (also called m1-toxin1) seems to act as a highly selective allosteric ligand of the M_1 receptor. Pharmacological studies of the MT7-hM_1 interaction report that MT7 blocks the subsequent interaction of [^{3}H]NMS with this receptor for several hours, fails to elicit a complete inhibition of the binding of orthosteric ligands, and significantly decreases or increases the dissociation rate of [^{3}H]NMS and [^{3}H]ACh, respectively (Max et al., 1993; Olianas et al., 2000, 2004; Krajewski et al., 2001; Mourier et al., 2003). However, all of these studies were done indirectly, and the mode of action of this toxin with M_1 receptor is not yet fully understood.

In this article, we first describe the iodination of synthetic MT7ox toxin and the complete physicochemical and pharmacological characterization of the interaction of an oxidized form of monoiodinated toxin with hM_1 receptor in the free and NMS-occupied states. Thus, for the first time, the affinity constants of the MT7ox-hM1 interaction were measured precisely by equilibrium and kinetic experiments using labeled MT7ox as radiotracer. In addition, the negative cooperativity between MT7ox and NMS was evaluated directly by the comparison of the toxin's affinities in the free and liganded receptor states. Furthermore, the effect of various orthosteric and allosteric agents on the dissociation kinetics of ^{125}I-MT7ox tracers was measured and sheds new light on the mode of interaction of these ligands when this toxin is used as radiotracer. The pharmacological profiles of various ligands were compared using ^{125}I-MT7ox or [^{3}H]NMS as tracer, and the binding data were analyzed with the allosteric ternary complex model. Finally, the binding of the MT1 toxin to hM_1 receptor was studied using both radiotracers, thereby highlighting the nonidentical pharmacological properties of these two toxins with the same receptor.

Materials and Methods

Materials

[^{3}H]*N*-Methyl scopolamine ([^{3}H]NMS; 78 Ci/mmol) was from Amersham Biosciences (Orsay, France). Atropine, *N*-methyl scopolamine, gallamine, brucine, staurosporine, KT5720, and tacrine were from Sigma-Aldrich (St. Quentin-Fallavier, France). Automated chain assembly was performed on a standard Applied Biosystems 433 peptide synthesizer (Applied Biosystems, Foster City, CA).

Peptide Synthesis, Disulfide Bond Formation, and Protein Purification

Chemical synthesis, refolding, and purification of the modified toxins were carried out using the methods described previously for the synthesis of the muscarinic MT1 and MT7 toxins (Mourier et al., 2003). In brief, the toxins were synthesized using the 9-fluorenylmethoxycarbonyl-stepwise solid-phase method with dicyclohexylcarbodiimide/1-hydroxy-7-azabenzotriazole as coupling reagent and *N*-methyl pyrrolidone as solvent. After TFA, deprotection, and purification of the crude material, the reduced form of the pure modified synthetic toxins was subjected to an oxidative reaction using a mixture of reduced (GSH) and oxidized (GSSG) glutathione in the presence of guanidine hydrochloride (0.5 M). Finally, the toxins were purified by reversed-phase HPLC using a Vydac C18 column (250 × 10 mm) with a gradient of 40 to 60% of solvent B for 40 min (A, 0.1% TFA in H_2O; B, 60% acetonitrile and 0.1% TFA in H_2O) and analytically characterized. Mass determinations were performed on a Micromass Platform II (Micromass, Altrincham, UK).

Preparation of Met35(sulfoxide)MT7 Toxin

MT7ox was obtained by mild oxidation of the MT7 toxin with 0.18% hydrogen peroxide in 0.05 M acetic acid for 15 min at room temperature, and toxin concentration was approximately 0.5 mg/ml (Rusconi and Montecucchi, 1985). The oxidized derivative was purified by HPLC using an analytical RP-18 (10 × 4.5 cm) HPLC Chromolith-performance column (VWR International, Fontenay sous Bois, France) and elution conditions as described under *Radioiodination*. The derivative was analytically characterized, and its mass was determined by spectrometric mass analyses.

Radioiodination

Toxins were radioiodinated for 2 min using 0.7 IU of lactoperoxidase (EC 1.11.1.7) from bovine milk using 1 nmol of toxin and 0.5 mCi of carrier-free Na^{125}I (PerkinElmer Life and Analytical Sciences, Boston, MA), in 10 μl of H_2O_2 (diluted 1:50,000) and 30 μl of 20 mM phosphate buffer, pH 7.2. The monoiodinated toxins were purified using an analytical (10 × 0.45 cm) RP-18 Chromolith-performance column and a 20 to 40% acetonitrile gradient in 30 min (buffer A, aqueous 0.1% TFA; buffer B, 100% acetonitrile and 0.085% TFA) at a flow rate of 2 ml/min. All fractions were collected, and 10 μl of each of them was measured with a γ counter (1261 Multigamma; LKB Wallac, Little Chalfont, Buckinghamshire, UK). Two fractions containing labeled MT7 toxin were eluted, respectively, at 27 and 29% of acetonitrile. The different iodinated forms of MT7 toxin were isolated and analyzed by binding experiments. The concentration of the radiolabeled toxins was determined according to the specific activity of ^{125}I corresponding to 2200 dpm/fmol of monoiodotoxin, depending on the age of the radiolabeled toxin and by estimation of its biological activity (usually 80% for ^{125}I-MT7). The fractions containing pure monoiodinated MT7 were kept at 4°C after the addition of bovine serum albumin (1 mg/ml). A nonradioactive iodination was performed using identical experimental conditions (10 μl of a 40 μM solution of NaI in 10 μM NaOH), then radioiodination, and monoiodinated MT7 toxins were analyzed by mass analysis; the position of the modified residue was then determined by N-terminal protein sequencing.

Mass Analysis and Protein Sequencing

Mass determination was performed on a ESI-Ion Trap Esquire HCT (Bruker Daltonik GmbH, Bremen, Germany), with samples dissolved or diluted in MS solvent ($CH_3CN/H_2O/HCO_2H$, 50:50:0.1). For protein sequence analysis, samples were loaded and argon-dried on a Biobrene-coated filter and then submitted to N-terminal sequencing according to Edman chemistry on an automatic ABI 492HT/Procise peptide sequencer from Applied Biosystems.

CD Analysis

CD spectra were recorded on a Jobin Yvon CD6 spectropolarimeter. Measurements were routinely performed at 20°C in 0.1-cm pathlength quartz cells (Hellma, Plainview, NY) with a peptide concentration of 5.10^{-5} M in 5 mM sodium phosphate buffer, pH 7.4. Spectra were recorded in the 186- to 260-nm wavelength range. Each spectrum represents the average of four spectra.

CHO Cells and Membrane Preparation

Professors P. O. Couraud and A. D. Strosberg (Institut Cochin de Génétique Moléculaire, Paris, France) kindly provided CHO cells stably expressing the cloned human muscarinic M_1 receptor. The cells were grown in plastic Petri dishes (Falcon, Cowley, UK) which were incubated at 37°C in an atmosphere of 5% CO_2 and 95% humidified air in Ham's F-12 medium precomplemented with L-glutamine and bicarbonate (Sigma) supplemented with 10% fetal calf serum and 1% penicillin/streptomycin (Sigma). At 100% confluence, the medium was removed, and the cells were harvested using Versen buffer (PBS + 5 mM EDTA). They were washed with ice-cold phosphate buffer and centrifuged at 1700*g* for 10 min (4°C). The pellet was suspended in ice-cold buffer (1 mM EDTA, 25 mM sodium phosphate, and 5 mM $MgCl_2$, pH 7.4) and homogenized using an Potter-Elvehjem homogenizer (Fisher Scientific Labosi, Elancourt, France). The homogenate was centrifuged at 1700*g* for 15 min (4°C). The sediment was resuspended in buffer, homogenized, and centrifuged at 1700*g* for 15 min (4°C). The combined supernatants were centrifuged at 35,000*g* for 30 min (4°C), and the pellet was suspended in the same buffer (0.1 ml/dish). Protein concentrations were determined according to the Lowry method using bovine serum albumin as standard. The membrane preparations were aliquoted and stored at −80°C.

^{125}I-MT7 Binding Assays

All binding experiments were done at room temperature in 10 mM sodium phosphate, pH 7.2, 135 mM NaCl, 2.5 mM KCl, pH 7.4 (PBS), and 0.1% bovine serum albumin. The reaction was stopped by addition of 2 × 3 ml of ice-cold buffer (PBS) immediately followed by filtration through GF/C glass-fiber filters (Whatman, Clifton, NJ) presoaked in 0.5% polyethylenimine. The bound radioactivity was counted in a γ counter (LKB 1261 multigamma). Nonspecific ^{125}I-MT7ox binding was determined in the presence of 100 nM MT7.

Saturation binding assays with unliganded receptor were performed by incubating CHO M_1 membrane (0.2 μg of protein/ml) for 18 to 20 h with increasing concentrations of ^{125}I-MT7ox (1–330 pM). For NMS-occupied receptor binding experiments, CHO M_1 membrane (6.5 μg of protein/ml) was first preincubated for 1 h with NMS (1 μM) and then for 18 to 20 h with varied concentrations of ^{125}I-MT7ox (40 pM to 2 nM). These NMS-occupied experimental conditions were determined by examining first the residual ^{125}I-MT7ox specific binding in function of increasing NMS concentrations. NMS concentrations up to 0.1 μM were associated with a constant ^{125}I-MT7ox specific binding. At 1 μM (10,000 times and 150 times its K_d for unliganded and MT7-occupied receptors, respectively), the receptor occupancy by NMS could not be reduced significantly, even with high ^{125}I-MT7ox concentrations. The association and dissociation kinetic experiments with ^{125}I-MT7ox were performed on free and NMS-occupied receptors. For both receptor states, the association kinetics were determined using four different concentrations of ^{125}I-MT7ox: 7, 12, 18, and 25 pM for unliganded receptor and 54, 110, 250, and 490 pM for NMS-occupied receptor (means ± S.E.M., $n = 3$). For dissociation experiments, after an 18- to 20-h preincubation of the free or NMS-occupied receptor with the radioligand, dissociation was monitored after the addition of 100 nM MT7. Aliquots were filtered and counted at different times (means ± S.E.M., $n = 6$).

To study the effect of various ligands on the dissociation kinetics of ^{125}I-MT7ox, hM_1 membranes were first preincubated 18 to 20 h with 20 pM ^{125}I-MT7ox, and then its dissociation was monitored after the addition of saturating concentrations of orthosteric or allosteric compounds (100 times their K_{dx} for free receptor) with 100 nM MT7 toxin. Aliquots were filtered and counted at different times. ^{125}I-MT7ox dissociation data were analyzed assuming a monoexponential decay equation.

The affinities of MT7, MT1 toxins, and various orthosteric and allosteric agents for muscarinic receptors were determined in inhibition binding experiments using ^{125}I-MT7ox as a tracer. The ^{125}I-MT7ox inhibition assays with free receptors used 15 pM ^{125}I-MT7ox, 0.2 μg of protein/ml, and overnight incubation, whereas 50 pM ^{125}I-MT7ox, 6.5 μg of protein/ml, and 6-h incubation were used for NMS-occupied receptors. For NMS-occupied receptor binding experiments, CHO M_1 membrane (6.5 μg of protein/ml) was first preincubated for 1 h with NMS (1 μM).

Each experiment was done at least three times. For ligands dissolved in DMSO (brucine, staurosporine, and KT5720), we checked that the higher concentration of DMSO present in the binding solution (2%) had no effect on the tracer binding.

[^{3}H]NMS Binding Assays

The effect of MT7 on the equilibrium binding of [^{3}H]NMS was determined in heterologous inhibition experiments. With [^{3}H]NMS as tracer, membrane protein concentrations, adjusted so that no more than 10% of added radioligand was specifically bound (around 1500–2000 cpm), were incubated in PBS-bovine serum albumin at 25°C for 18 to 22, with varying concentrations of toxin and [^{3}H]NMS (0.5 nM) in a final assay volume of 300 μl. Nonspecific binding was determined in the presence of 50 μM atropine. The reaction was stopped by the addition of 3 ml of ice-cold buffer (PBS) immediately followed by filtration through Whatman GF/C glass-fiber filters presoaked in 0.5% polyethylenimine. The filters were washed once again with 3 ml of ice-cold buffer (PBS), dried, and the bound radioactivity was counted by liquid scintillation spectrometry. Each experiment was done at least three times.

Data Analysis

The binding data from individual experiments ($n \geq 3$) were analyzed by nonlinear regression analysis using Kaleidagraph 4.0 (Synergy Software, Reading, PA).

Saturation Binding Experiments. The results from saturation binding experiments were subjected to nonlinear regression analysis to obtain the equilibrium dissociation constant (K_d) and the number of binding sites (B_{max}).

Inhibition Binding Experiments. After subtraction of the nonspecific binding and normalization, data obtained with [^{3}H]NMS and ^{125}I-MT7ox were analyzed using the Hill equation to estimate the IC_{50} and the slope factor, n_H, of the inhibition curve. The affinities of the orthosteric agents in inhibiting the binding of [^{3}H]NMS, expressed as pK_i, were calculated from the IC_{50} values by applying the Cheng-Prusoff correction (Cheng and Prusoff, 1973). K_d value of the [^{3}H]NMS on hM_1 receptor was experimentally determined by saturation experiments and was equal to 0.1 nM, as reported previously in the literature (Matsui et al., 1995; Lu et al., 2001). Likewise, the affinities of the muscarinic toxins in inhibiting the binding of ^{125}I-MT7ox to free or liganded receptors were expressed as pK_i values.

The allosteric ternary complex model (Ehlert, 1988) was used to analyze the data on the effect of orthosteric and allosteric agents on the specific binding of the allosteric radioligand ^{125}I-MT7ox and of the allosteric agents on the specific binding of the orthosteric radioligand [^{3}H]NMS. We used the following equation (Lazareno and Birdsall, 1995):

$$B_{LX} = B_o \times \frac{(1 + [L] \times K_L) \times (1 + \alpha \times (K_X \times [X])^{n_H})}{1 + (K_X \times [X])^{n_H} + [L] \times K_L \times (1 + \alpha \times (K_X \times [X])^{n_H})} \quad (1)$$

B_{LX} denotes the specific binding of the respective radioligand L (either [^{3}H]NMS or ^{125}I-MT7ox) in the presence of the cooperatively interacting agent X (allosteric or orthosteric agents). B_o is the bind-

ing of L in the absence of X. K_L and K_x are the affinity constants for the binding of L and X, respectively, to the unliganded receptors. α Denotes the cooperative factor for the allosteric interaction between X and L (with $\alpha > 1$, $\alpha < 1$, $\alpha = 1$ indicating positive, negative, and neutral cooperativity, respectively). n_H represents the slope factor of the curve.

The positive cooperativity of KT5720 with ^{125}I-MT7ox may be associated, at high KT5720 concentration, with slow kinetics of ^{125}I-MT7ox binding that prevents equilibrium from being reached. In that case, the binding data were better fitted with the following equation, which assumes that the modulator completely prevents the dissociation of radioligand from the receptor (Lazareno and Birdsall, 1995; Lazareno et al., 2000):

$$B_{LXt} = B_{LX} \times \left(1 - \exp\left(\frac{-t \times k_{off}}{1 + \alpha \times (K_X \times [X])^{n_H}} + \frac{-t \times k_{off} \times [L] \times K_L}{1 + (K_X \times [X])^{n_H}}\right)\right) \quad (2)$$

where B_{LXt} is the observed specific binding under nonequilibrium conditions, B_{LX} is the predicted equilibrium binding defined in eq. 1, t is the incubation time, and k_{off} is the dissociation rate constant of ^{125}I-MT7ox.

Results

Chemical Synthesis, Refolding, Purification, and CD Spectra Analyses of Wild-Type and Modified MT7 Toxins. The one-step, solid-phase chemical syntheses of the natural and modified MT7 toxins were performed using a program developed previously for the synthesis of nicotinic and muscarinic toxins (Mourier et al., 2000, 2003). For each toxin, the synthesis proceeded smoothly, and the final TFA cleavage yielded a crude mixture in which the main component, corresponding to the reduced form of each protein, constituted 30 to 40% of the total reaction mixture analyzed by reversed-phase HPLC. Refolding of these toxins was performed in the presence of reduced and oxidized glutathione and 0.5 M guanidine hydrochloride, and the final oxidation yield was approximately 30%. The refolded modified synthetic MT7 toxins were purified to homogeneity on a C18 reversed-phase HPLC column. The purity and identity of the toxins was confirmed by electrospray mass analysis. Finally, the CD spectra of the different synthetic toxins were recorded and displayed a typical β-sheet signature with pronounced maxima and minima at 194 to 196 and 210 to 216 nm, respectively (data not shown) as described previously (Mourier et al., 2003).

Iodination of MT7 Toxin and Kinetic Binding Experiments of Labeled Derivatives. To obtain a high specific-activity ligand that interacts with the allosteric site of the hM_1 receptor, MT7 toxin was monoiodinated under mild conditions using the lactoperoxidase method and a 1:5 $Na^{125}I$/protein ratio (as described under *Materials and Methods*). After the reaction, the resulting products were separated by C18 reversed-phase HPLC chromatography (Fig. 1). As shown in Fig. 1A, the chromatogram displays the presence of a major peak at a retention time (RT) of 13.2 min corresponding to the unmodified MT7 toxin (experimental mass, 7472.9) and three minor peaks: a, RT, 10.9 min; mass, 7488.4 (+15.5); b, RT, 12.2 min; mass, 7614.2 (+141.3); and c, RT, 14.3 min; mass, 7598.6(+125.7), corresponding, respectively, to an oxidized form of the MT7 toxin (peak a), its monoiodinated derivative (peak b), and the monoiodinated derivative of the wild-type MT7 toxin (peak c). According to the mild oxidative conditions used for the toxin iodination, the only residue likely to be oxidized is the sole methionine at position 35. To confirm the location of this oxidation, the same oxidative conditions were applied to an M35A modified toxin, which was unchanged by this treatment (data not shown). Thus, a Met35-sulfoxide derivative of the MT7 toxin was synthesized (as described under *Materials and Methods*), analyzed by mass spectrometry, and submitted to nonradioactive iodination. As shown in Fig. 1B, the HPLC profile obtained after nonradioactive iodination of MT7ox presents a major peak with a mass and an RT identical with that of peak a, corresponding to the unmodified MT7ox and a minor peak with a mass and an RT identical with those of peak b identified as a monoiodinated MT7ox toxin. After radioiodination of the wild-type toxin, the radioactivity was found for the most part in peak c (80%) and also in peak b (15%) (Fig. 1A′). MT7ox toxin was radioiodinated, and the radioactivity was entirely associated with the fraction at the RT of 12.2 min corresponding to the monoiodinated MT7ox toxin (called ^{125}I-MT7ox) (Fig. 1B′). Finally, the analysis of the first 40 cycles of the N-terminal protein sequencing of monoiodinated MT7 toxin indicated no modification at Tyr30 and Tyr36, assuming, in the absence of histidine residue, that iodination occurred on the third and last tyrosine residue in position 51. Dissociation kinetic experiments were performed first with the two radioiodinated MT7 peaks b and c using a free CHO hM_1 membrane preparation. As reported in Fig. 2A, a large fraction of peak c bound stably to the receptor. After more than 2 days of incubation, a large excess of nonradioactive MT7 displaced less than 40% of the labeled toxin. In contrast, dissociation of ^{125}I-MT7ox peak b from the receptor was complete and displayed a monoexponential relationship with a dissociation rate constant (k_{off}) of $3.3 \pm 0.2\ 10^{-3} \cdot min^{-1}$. Thus, all of the following experiments with labeled toxin were performed using the reversible peak b as tracer (^{125}I-

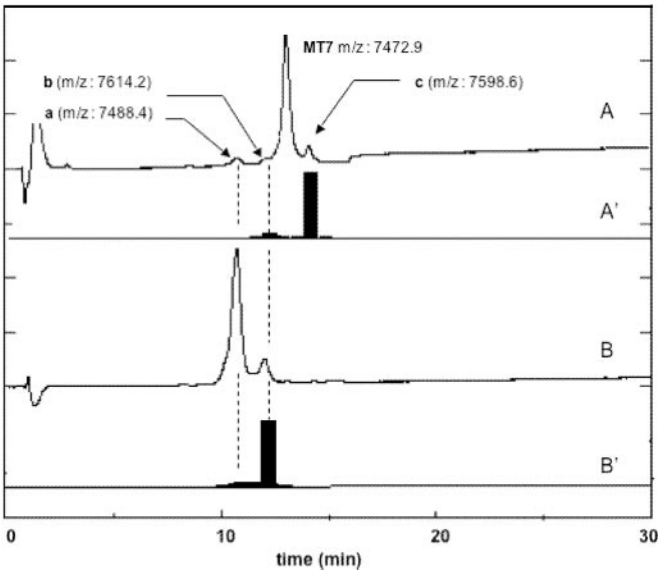

Fig. 1. Analytical HPLC profiles obtained after radioiodination and UV detection of MT7 (A) and MT7ox (B). A′ and B′ represent the corresponding relative radioactivity associated with each peak in the chromatogram. Reverse-phase HPLC conditions are described under *Results*. Mass was measured by spectrometric mass analysis and is indicated for each peak on the chromatogram.

MT7ox). The association rate constant (k_{on}) of this compound was determined using a constant concentration of membrane preparation and four different concentrations of the ^{125}I-MT7ox (Fig. 2B). The k_{on} value calculated from the linearization plot of K_{app} versus the ^{125}I-MT7ox concentrations (Fig. 2B, inset) was 2.5 ± 0.4 10^8 $M^{-1} \cdot min^{-1}$. Thus, the dissociation constant (K_d) calculated from the k_{off}/k_{on} ratio is equal to 13.2 ± 2.3 pM.

Binding of ^{125}I-MT7ox to Free and NMS-Occupied hM_1 Receptor. When CHO hM_1 membrane preparations were incubated for 18 to 20 h with increasing concentrations of ^{125}I-MT7ox, typical saturation binding curves were obtained (Fig. 3). Nonspecific binding was obtained in the presence of a large excess of MT7 (100 nM). A nonlinear analysis of these data indicates a K_d of 14.3 ± 3.1 pM and a B_{max} of 15.1 ± 2.8 pmol/mg of protein. Furthermore, linearization and Scatchard analysis confirms the presence of a single class of binding sites (data not shown). This dissociation constant agrees well with that determined by kinetic experiments.

Kinetic and saturation experiments were also performed with the NMS-occupied receptor, obtained after 1 h of preincubation of the CHO hM_1 membrane preparation with a large excess of NMS (1 μM). Association and dissociation constants calculated from their respective kinetic experiments (Fig. 4, A and B) are, for k_{on}, 1.52 ± 0.22 10^8 $M^{-1} \cdot min^{-1}$, and for k_{off}, 0.12 ± 0.01 min^{-1}, leading to an apparent affinity of the toxin on the NMS-occupied receptor, K_d^{occ}, of 0.79 ± 0.17 nM calculated from the k_{off}/k_{on} ratio. Saturation binding curves of ^{125}I-MT7ox on a liganded receptor (Fig. 5) indicated a K_d^{occ} of 0.92 ± 0.02 nM, a value similar to that given by kinetic experiments, and a B_{max} of 10.6 ± 1.4 pmol/mg of protein. Thus, a large decrease of the affinity of the ^{125}I-MT7ox toxin for the hM_1 receptor was observed in its NMS-occupied state compared with its unliganded state, revealing a negative cooperativity between these two ligands, associated with a cooperative factor α = 0.015 calculated from the ratio of the apparent affinity constant values of the^{125}I-MT7ox for the free (0.0143 nM) and NMS-occupied (0.92 nM) receptors.

To complete the direct characterization of the MT7-hM1 interaction, competitive binding experiments on ^{125}I-MT7ox and wild-type MT7 with free and NMS-occupied receptor were performed. Figure 6 shows the two inhibition binding curves obtained with, in both cases, a complete displacement of the tracer by the MT7 toxin. The affinity constants (K_i) deduced from these competition binding curves using the Cheng-Prusoff equation of 11.6 ± 1.5 pM (pK_i = 10.95 ± 0.01) and 1.7 ± 0.2 nM (pK_i = 8.75 ± 0.05) for the free and NMS-occupied receptor, respectively, are very similar to those determined from saturation or kinetic experiments. In addition, ^{125}I-MT7ox binding was inhibited with the nonradioactive iodinated oxidized toxin, and the calculated K_i constants with free or NMS-occupied receptors are similar to those obtained with the wild-type MT7 of 18.62 ± 0.35 pM (pK_i = 10.73 ± 0.13) and 2.72 ± 0.12 nM (pK_i = 8.57 ± 0.02), respectively (data not shown).

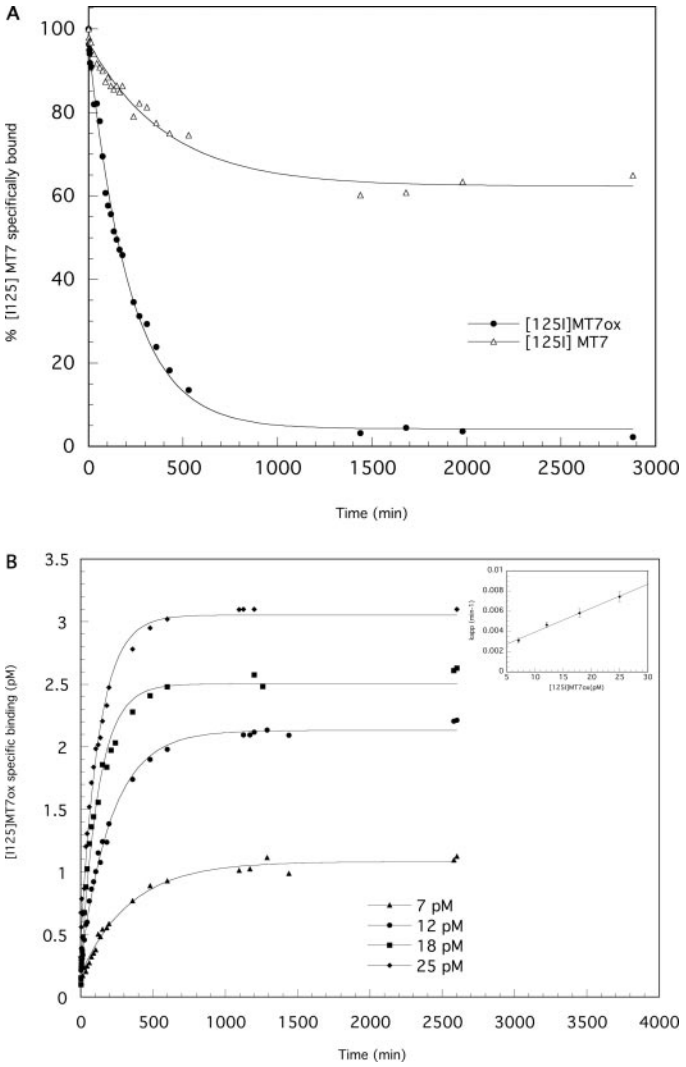

Fig. 2. A, dissociation kinetics of wild-type and MT7ox monoiodinated toxins with free hM_1 receptor. After 18- to 20-h preincubation of the receptor with the labeled toxin, the dissociation was monitored after the addition of 100 nM MT7, and aliquots were filtered and counted at different times. Data are from one experiment repeated six times. B, association kinetics of ^{125}I-MT7ox at four different concentrations: 7, 12, 18, and 25 pM with unliganded receptor. Inset, linearization of the different K_{app} association constants as a function of tracer concentration. Data are from one experiment repeated three times.

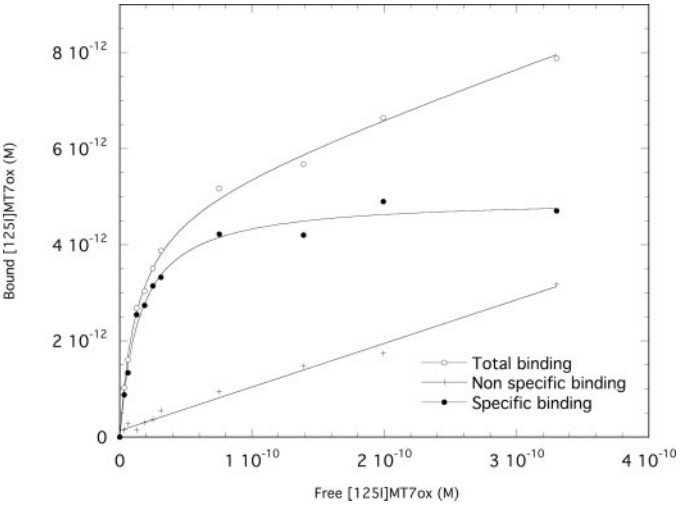

Fig. 3. Saturation binding assays of ^{125}I-MT7ox with unliganded receptor. CHO M_1 membrane (0.2 μg of protein/ml) was incubated for 18 to 20 h with increasing concentrations of ^{125}I-MT7 (1–330 pM) alone (total binding) or with a large excess of nonradioactive toxin (nonspecific binding). Specific binding was obtained by subtracting nonspecific binding from total binding. Data are from one experiment repeated three times.

Effect of Allosteric and Orthosteric Ligands on ^{125}I-MT7ox Dissociation Kinetics. To characterize the type of interaction of different ligands with ^{125}I-MT7ox-hM$_1$ binding, the effect of these various ligands on MT7-induced ^{125}I-MT7ox dissociation was investigated. As shown in Fig. 7, the test compounds induce different types of effects on ^{125}I-MT7ox dissociation. First, KT5720 slows down the dissociation kinetics weakly but significantly (Table 1), whereas atropine, NMS, staurosporine, and mostly gallamine, brucine, and tacrine increase the ^{125}I-MT7ox dissociation rate constants from 2- to 100-fold (Table 1). For example, tacrine induces a complete ^{125}I-MT7ox dissociation in a few minutes compared with the $t_{1/2}$ dissociation of 3.5 h obtained with MT7 toxin alone. Thus, because modification of radioligand dissociation by a test compound demonstrates its allosteric behavior, all of the ligands studied can be considered allosteric modulators of the ^{125}I-MT7ox-hM$_1$ interaction. In contrast, MT1 toxin does not affect the MT7 dissociation rate (Fig. 7), suggesting a competitive interaction between the two toxins even if a high negative cooperativity could not be excluded.

Inhibition of ^{125}I-MT7ox Binding to Free hM$_1$ Receptor by Various Allosteric and Orthosteric Ligands. Specific ^{125}I-MT7ox binding to free receptor was inhibited by increasing concentrations of various ligands as the orthosteric antagonists, NMS and atropine, or the allosteric agents gallamine, brucine, tacrine, staurosporine, and KT5720 (Fig. 8A). At the higher concentrations of NMS and atropine, the ^{125}I-MT7ox binding was not completely abolished, indicating a negative cooperative interaction of these antagonists with the allosteric tracer. According to the ternary complex model, if such cooperative interaction occurred, the derived affinity

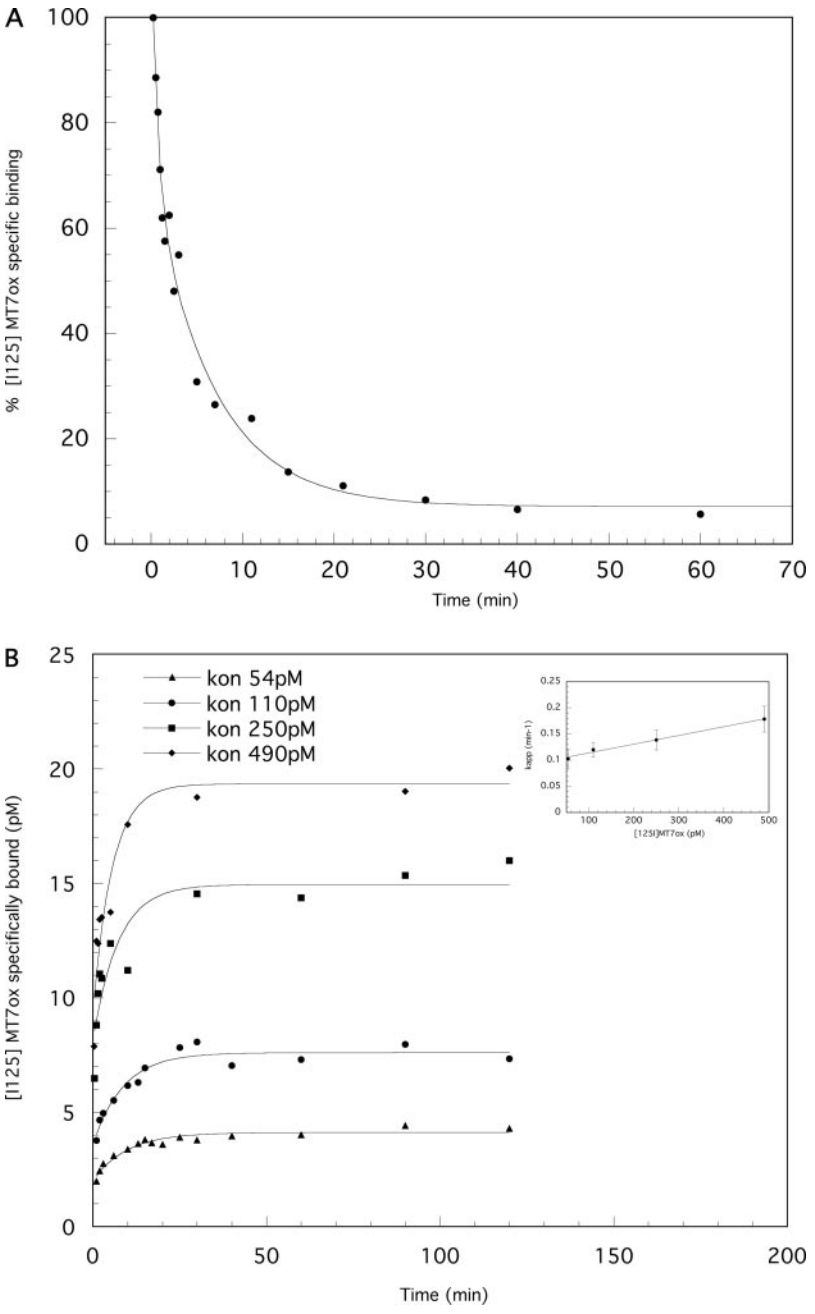

Fig. 4. A, dissociation kinetics of ^{125}I-MT7ox toxin with NMS-occupied hM$_1$ receptor. CHO hM$_1$ membrane was first saturated for 1 h with 1 μM NMS and then incubated for 18 to 20 h with the labeled toxin. Dissociation was monitored after the addition of 100 nM MT7, and aliquots were filtered and counted at different times. B, association kinetics of ^{125}I-MT7ox at four different concentrations: 54, 110, 250, and 490 pM with NMS-occupied receptor. Inset, linearization of the different K_{app} association constants as a function of tracer concentration. Data are from one experiment repeated three times.

constants for the unliganded receptor should match those obtained in inhibition binding experiments with [^{3}H]NMS. The slope factors measured in these experiments are not significantly different from the unity, and the affinity constants of these two ligands are in the subnanomolar range (Table 2). For the allosteric agents, a complete radiotracer displacement was observed with brucine, tacrine, and staurosporine but not with gallamine, whereas with KT5720, the ^{125}I-MT7ox binding first increased by 35% at 6 μM and then decreased at higher concentrations (Fig. 8A). The KT5720 complex binding curve may reflect a kinetic artifact of high concentrations of this agent on the ^{125}I-MT7ox binding and was fitted according to a kinetic ternary complex equation (see eq. 2 under *Materials and Methods*). Depending on the allosteric properties of these agents observed in ^{125}I-MT7ox dissociation experiments, their affinity constants (log Kx = $-$pK_x) reported in Table 2 were derived from the treatment of the inhibition binding curves with the ternary complex equation. All of these ligands are characterized by affinity constants in the micromolar range (Table 2).

In equilibrium binding experiments with MT1 toxin, ^{125}I-MT7ox binding to free M_1 receptor was completely inhibited by MT1 (Fig. 8B) and associated with a pK_i = 7.58 ± 0.03 obtained by competitive treatment of the binding curve using the Cheng-Prusoff equation. Thus, MT1 interacts with the hM_1 receptor with an affinity 3 orders of magnitude lower than that of MT7 (Table 2).

Inhibition of [^{3}H]NMS Binding to Free hM_1 Receptor by Various Allosteric and Orthosteric Ligands. Equilib-

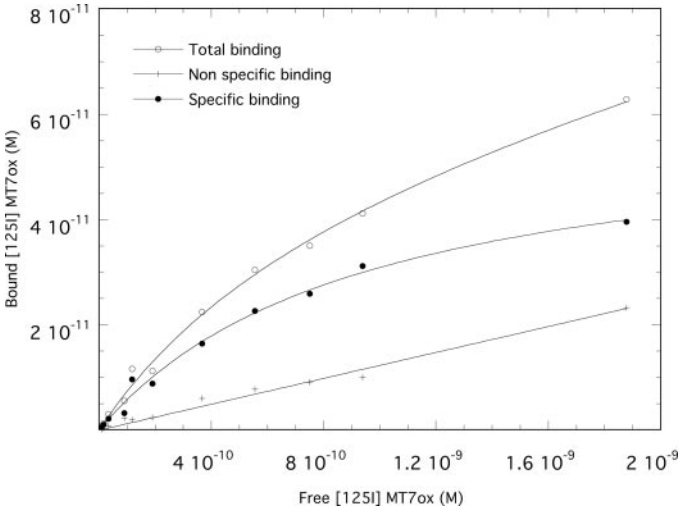

Fig. 5. Saturation binding assays of ^{125}I-MT7ox with NMS-occupied receptor. CHO M_1 membrane (6.5 μg of protein/ml) was first preincubated for 1 h with NMS (1 μM) and then incubated for 18 to 20 h with increasing concentrations of ^{125}I-MT7ox (40 pM to 2 nM) alone (total binding) or with a large excess of nonradioactive toxin (nonspecific binding). Specific binding was obtained by subtracting nonspecific binding from total binding. Data are from one experiment repeated three times.

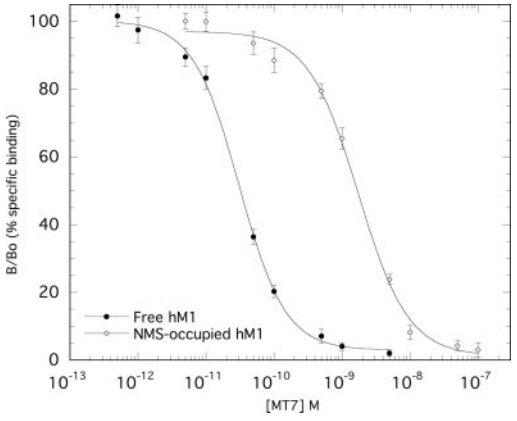

Fig. 6. Inhibition of ^{125}I-MT7ox-specific binding by wild-type MT7 toxin on free or NMS-occupied M_1 receptor. Binding experiments were performed by 18- to 20-h incubation of varying concentrations of wild-type MT7 with ^{125}I-MT7ox (15 pM) and free membrane receptors (0.2 μg of protein/ml) or by 18- to 20-h incubation of 50 pM ^{125}I-MT7ox and NMS-occupied receptor (6.5 μg of protein/ml, preincubated for 1 h with 1 μM NMS). Curves were fitted using the Hill equation. Data are mean values ± S.E.M. of at least five inhibition binding experiments.

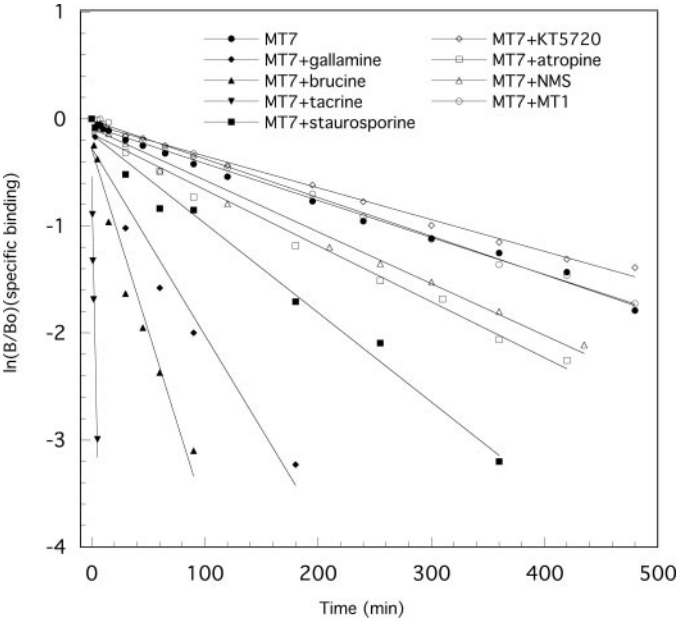

Fig. 7. Kinetics of the dissociation of ^{125}I-MT7ox from M_1 receptor monitored after the addition of MT7 alone or in combination with various ligands. hM_1 membranes were preincubated for 18 to 20 h with 20 pM ^{125}I-MT7ox and then with the addition of 100 nM MT7 toxin, with or without saturating concentrations of orthosteric or allosteric compounds (1 μM NMS and atropine, 2 μM MT1, 5 μM KT5720, 10 μM staurosporine and gallamine, and 1 mM brucine and tacrine) prevent its reassociation, thus allowing dissociation to be monitored over time. Iodinated MT7ox dissociations were analyzed assuming a monoexponential decay equation and expressed on a semilogarithmic scale, where B and B_o represent the specific binding at times t and t_o, respectively. Data are from one experiment repeated three times.

TABLE 1

Kinetic parameters of ^{125}I-MT7ox dissociation from hM_1 receptor induced by MT7 toxin alone or in combination with various orthosteric and allosteric ligands

CHO hM_1 membranes were first preincubated for 18 to 20 h with 20 pM ^{125}I-MT7ox, and then dissociation was initiated by 100 nM MT7 toxin with or without saturating concentrations of orthosteric or allosteric compounds. K_{off} values are the mean ± S.E.M. of three to five experiments.

Ligands	K_{off}
	$min^{-1} \times 10^{-3}$
MT7	3.3 ± 0.3
MT7 + gallamine	14 ± 2
MT7 + brucine	34 ± 5
MT7 + tacrine	310 ± 22
MT7 + staurosporine	8.6 ± 0.5
MT7 + KT5720	2.7 ± 0.3
MT7 + NMS	4.7 ± 0.5
MT7 + atropine	5.2 ± 0.2
MT7 + MT1	3.1 ± 0.3

rium experiments were performed using [^{3}H]NMS as a tracer for allosteric ligands shown previously to interact at different sites on the hM_1 receptor. According to the allosteric ternary complex model, these ligands should have a cooperative effect on the binding of an orthosteric agent, such as [^{3}H]NMS. Results of the equilibrium assays with unliganded receptor showed a negative cooperativity of MT7, gallamine, brucine, and tacrine in [^{3}H]NMS binding, and the inhibition binding curves did not reach zero radioligand binding (Fig. 9A). Table 2 gives the affinity constants (log $Kx = -pK_x$) for the interaction of these allosteric ligands with unliganded receptor and the cooperativity factors associated with the quantitative analysis of these interactions according to the ternary complex model (eq. 1).

The effects of orthosteric ligands, such as NMS and atropine, on [^{3}H]NMS binding are illustrated in Fig. 9B, and the equilibrium binding parameters are reported in Table 2. The pK_i ($-\log K_i$) constants from these competition experiments were calculated from their IC_{50} values by applying the Cheng-Prusoff equation. The slopes of these curves did not deviate from unity. In view of the lack of effect of the MT1 toxin, in our experimental conditions, on the [^{3}H]NMS dissociation kinetics (Mourier et al., 2003), its competitive binding curve was treated as for classic orthosteric ligands (Table 2).

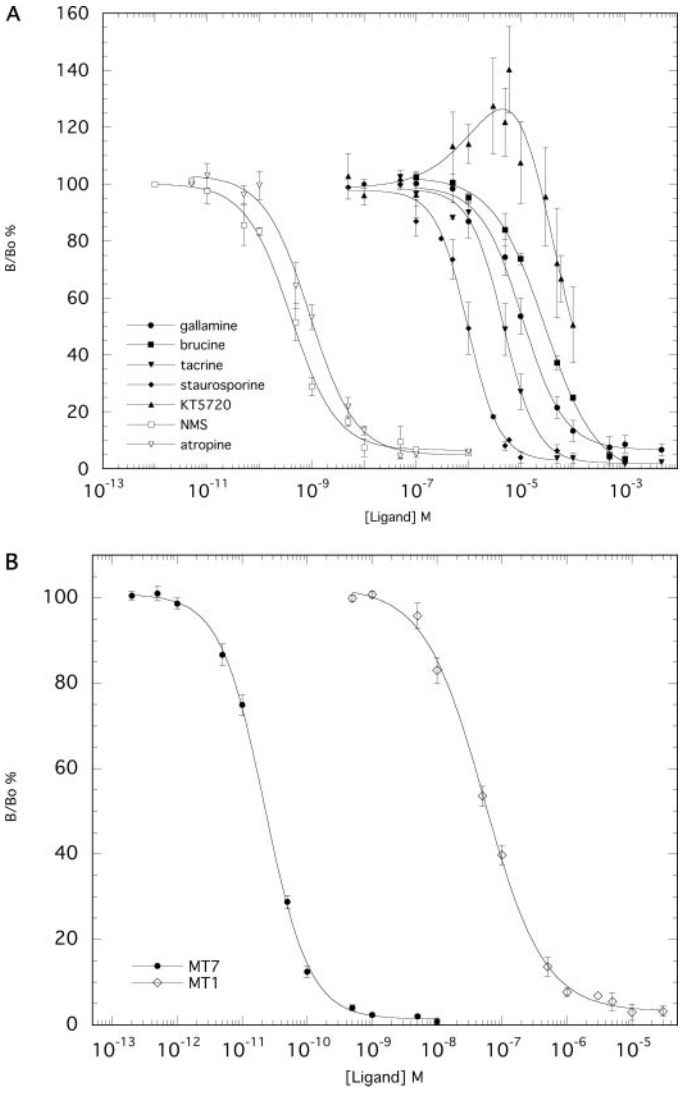

Fig. 8. Inhibition of specific ^{125}I-MT7ox binding by increasing concentrations of various ligands. A, effect of allosteric and orthosteric ligands on ^{125}I-MT7ox binding to free hM_1 receptor. Nonspecific binding of the radiotracer was defined in the presence of 100 nM MT7, and the specific binding of ^{125}I-MT7ox (15 pM) in the absence of ligands was set at 100%. The curve fits were based on the ternary complex equation (eq. 1), except for the complex KT5720 binding curve, which was fitted according to the kinetic ternary complex equation (eq. 2) reported under *Materials and Methods*. Data are mean values ± S.E.M. of three to five inhibition experiments. B, effect of MT7 and MT1 toxins on ^{125}I-MT7ox binding to free hM_1 receptor. The results are expressed as the ratio of the specific ^{125}I-MT7ox binding measured with (B) or without (B_o) the different toxins. Curve fitting was based on a nonlinear regression analysis using the Hill equation. Data are mean values ± S.E.M. of at least three inhibition experiments.

Discussion

With the exception of the [^{3}H]dimethyl-W84 radiotracer, which binds to the allosteric site on the hM_2 receptor and has recently been used to characterize the interaction of various ligands with this receptor subtype (Trankle et al., 2003), all of the interactions of allosteric agents with muscarinic receptors have been inferred from their indirect effects on the kinetics or equilibrium binding of orthosteric radioligands, principally [^{3}H]NMS. Thus, to characterize directly the interaction of the hM1 receptor with selective allosteric MT7 toxin, we radioiodinated this toxin in select conditions that generate a high-affinity iodinated toxin that binds reversibly and characterized it pharmacologically. Furthermore, this allosteric radiotracer was used to determine the binding constants of various orthosteric and allosteric ligands, allowing a comparison with results previously obtained using [^{3}H]NMS.

The enzymatic radioiodination of MT7 and the mild oxidative conditions used in this labeling process generate two MT7 toxins derivatives, monoiodinated on Tyr51 and with or without a sulfoxidation on Met35 residue. The dissociation kinetics of these two molecules have been performed, and their profiles differ widely. Thus, the monoiodinated MT7 binds quasi-irreversibly on the hM_1 receptor, whereas the dissociation of the ^{125}I-MT7ox displays a monoexponential relationship with a complete dissociation at equilibrium (Fig. 2A). These results confirm the huge stability of the MT7-hM_1 interaction, as it was identified previously with [^{3}H]NMS binding (Max et al., 1993; Olianas et al., 2000; Krajewski et al., 2001; Mourier et al., 2003), and suggest that the oxidation of the Met35 significantly destabilizes this interaction. This property was confirmed by studying the stability of the toxin-receptor complexes, evaluated by the [^{3}H]NMS association kinetic performed after toxin preincubation. In these experiments, wild-type MT7 completely blocks the [^{3}H]NMS binding, whereas preincubation with MT7ox allows efficient binding of [^{3}H]NMS (in 2 h, 60% of the binding control level, data not shown). Furthermore, the alteration of the stability of the MT7-hM_1 interaction, without a significant effect on the apparent toxin affinity constant, has been observed previously with the F38I mutant (Krajewski et al., 2001).

Thus, ^{125}I-MT7ox toxin interacts reversibly with the hM_1 receptor and was used as radiotracer in association/dissociation, saturation, and competition experiments to fully characterize the interaction of MT7ox toxin with free and NMS-occupied hM_1 receptor.

The affinity constants of ^{125}I-MT7ox toxin, obtained from kinetic experiments, are equal to 13.20 ± 2.3 pM and 0.79 ±

TABLE 2

Equilibrium binding parameters of the interaction of orthosteric and allosteric ligands on free hM_1 muscarinic receptor using ^{125}I-MT7ox and [^{3}H]NMS as tracers

Data are the mean ± S.E.M. of three to six different experiments according to the procedure described under *Materials and Methods*. The treatments of the curves are detailed in *Data Analysis*.

	[^{125}I]MT7ox				[^{3}H]NMS			
	pK_i	log K_x	n_H	α	pK_i	log K_x	n_H	α
MT7	10.95 ± 0.01		1.23 ± 0.05			10.53 ± 0.08	1.06 ± 0.12	0.014 ± 0.004
Gallamine		5.28 ± 0.27	1.08 ± 0.13	0.031 ± 0.009		5.48 ± 0.06	0.96 ± 0.04	0.052 ± 0.006
Tacrine		5.58 ± 0.14	1.36 ± 0.17	0.009 ± 0.006		5.79 ± 0.04	1.23 ± 0.05	0.011 ± 0.004
Brucine		4.95 ± 0.07	0.98 ± 0.07	0.015 ± 0.003		4.58 ± 0.05[a]		0.91 ± 0.04[a]
Staurosporine		6.29 ± 0.11	1.43 ± 0.18	0.012 ± 0.008		5.91 ± 0.03[b]	1.01 ± 0.01[b]	1.53[b]
KT5720		5.67 ± 0.34	0.83 ± 0.09	2.79 ± 0.31		6.42 ± 0.09[b]	1.00[b]	1.94[b]
NMS		9.92 ± 0.06	1.01 ± 0.09	0.012 ± 0.006	9.94 ± 0.03		0.97 ± 0.08	
Atropine		9.38 ± 0.15	1.00 ± 0.06	0.014 ± 0.006	9.31 ± 0.02		0.92 ± 0.10	
MT1	7.58 ± 0.03		0.94 ± 0.06		7.63 ± 0.04		0.90 ± 0.05	

[a] Data from Lazareno et al. (1998).
[b] Data from Lazareno et al. (2000).

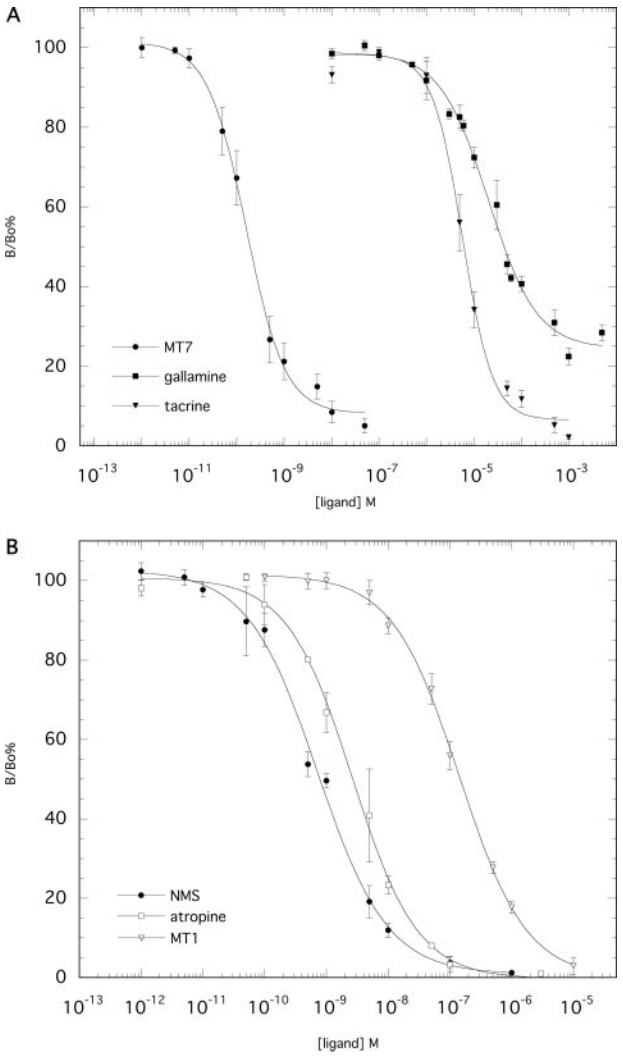

Fig. 9. A, effect of allosteric agents on [^{3}H]NMS equilibrium binding to free hM_1 receptor. [^{3}H]NMS (0.5 nM) was incubated with CHO-M1 membrane for 18 to 22 h in the presence and absence of increasing concentrations of allosteric ligands. Nonspecific binding was determined in the presence of 50 μM atropine. The curve fits were based on the ternary complex equation reported in the experimental part. B, inhibition of the specific binding of [^{3}H]NMS by increasing concentrations of orthosteric ligands and MT1 toxin. Curve fitting was based on a nonlinear regression analysis using the Hill equation. The results are expressed as the ratio of the specific ^{125}I-MT7ox binding measured with (B) or without (B_o) the different toxins. Data are mean values ± S.E.M. of at least three inhibition experiments.

0.17 nM with unliganded and NMS-occupied receptor, respectively. Thus, the calculated cooperative factor is 0.016. With saturation experiments, similar values of 14.26 ± 3.13 pM and 0.92 ± 0.02 nM were obtained, respectively, associated with a cooperative factor of 0.015. The number of toxin binding sites calculated from saturation experiments is 15.1 ± 2.8 pmol/mg of protein and 10.6 ± 1.4 pmol/mg of protein in free and liganded receptor states, respectively. In NMS-occupied receptor, this value is probably underestimated because of the impossibility of totally saturating the receptor in these experimental conditions. In competition binding experiments using monoiodinated MT7ox as tracer, inhibition constants of wild-type MT7 toxin with free and NMS-occupied receptor were, respectively, 11.6 ± 1.5 pM (pK_i = 10.95 ± 0.01) and 1.7 ± 0.2 nM (pK_i^{occ} = 8.75 ± 0.05), confirming the huge negative allosteric effect of NMS on ^{125}I-MT7ox binding. This effect was mainly supported by a dramatic increase in ^{125}I-MT7ox dissociation in the NMS-occupied receptor ($t_{1/2}$ = 5 min) compared with the unliganded receptor ($t_{1/2}$ = 3.5h) (Figs. 2A and 4A), with the association kinetics being highly similar (Figs. 2B and 4B). Furthermore, a similar negative cooperativity (α = 0.014) between NMS and MT7 was calculated when [^{3}H]NMS was used as tracer and the inhibition binding curves were treated with the ternary complex eq. 1 (Table 2). In this model, the affinity of the MT7 for the free receptor is 29 ± 3 pM (pK_x = 10.53 ± 0.08) similar to that obtained from ^{125}I-MT7ox competition experiment (Table 2). Furthermore, the affinity of the MT7 for the NMS-occupied receptor can be calculated as $\log(\alpha \cdot Kx) = -pK_x^{occ} = 8.67$, and this value agrees well with the experimental affinity of the MT7 for the NMS-occupied receptor measured previously with single-time point experiments (pK_i^{occ} = −log IC_{50}^{diss} = 8.60 ± 0.04) (Mourier et al., 2003). Thus, the similarity of the binding constants and cooperativity factors of the MT7-hM_1 receptor interaction measured directly using ^{125}I-MT7ox or indirectly with [^{3}H]NMS validates the ternary complex model in studying the interaction of two ligands that interact with separate but conformationally linked sites on a receptor and confirm the reciprocal nature of the cooperativity. Furthermore, the identity of the B_{max} values obtained with saturation experiments using ^{125}I-MT7ox (15.1 ± 2.8 pmol/mg of protein) or [^{3}H]NMS (16.4 ± 3.3 pmol/mg of protein, data not shown) suggests that the number of binding sites on the hM_1 receptor for the allosteric toxin or the orthosteric ligand is identical.

It was possible to demonstrate that different orthosteric and allosteric ligands significantly modified the dissociation kinetics of ^{125}I-MT7ox (Fig. 7), particularly tacrine, brucine, and gallamine, which drastically accelerated them (Table 1). In contrast, KT5720 decreased the ^{125}I-MT7ox dissociation rate, in agreement with a positive allosteric effect. These observations were confirmed in equilibrium binding studies with the different orthosteric and allosteric agents, in which the negative or positive cooperative factors calculated with the ternary complex equation (Table 2) agreed well with their respective increase or decrease effects on ^{125}I-MT7ox dissociation. It is interesting to note that although the modification of radiotracer dissociation by a test ligand unambiguously demonstrates its allosteric properties, this kind of experiment does not quantitatively evaluate the cooperativity of this interaction. This is particularly clear for the ^{125}I-MT7ox-NMS-hM1 ternary complex, in which the NMS only weakly (40%) accelerates the MT7-induced ^{125}I-MT7ox dissociation (Table 1), whereas in direct binding experiments, the ^{125}I-MT7ox k_{off} constant is drastically increased (45-fold) in NMS-occupied receptor compared with its free state.

Furthermore, the log affinities of several allosteric ligands, determined from their inhibition of the specific binding of ^{125}I-MT7ox to unliganded receptor, agreed with those obtained from allosteric binding with [^{3}H]NMS (Table 2). For gallamine and tacrine, these affinity constants are highly similar to those reported in the literature (Potter et al., 1989; Lee and el-Fakahany, 1991; Matsui et al., 1995). The steepness of the binding curve for tacrine observed with ^{125}I-MT7ox also has been reported previously with [^{3}H]NMS (Potter et al., 1989; Trankle et al., 2005) and suggests that tacrine may interact with an allosteric site distinct from that of classic allosteric agents. For brucine, the experimental pK_x value obtained with ^{125}I-MT7ox (4.95 $\pm$ 0.07) is similar to the literature value determined by quantitative equilibrium assay measuring the inhibition of [^{3}H]NMS binding by ACh in the presence of brucine (4.58 $\pm$ 0.05) (Lazareno et al., 1998). In addition, the interaction of two indolocarbazole compounds, staurosporine and KT5720, previously identified as positive allosteric modulators of [^{3}H]NMS on hM1 receptor (Lazareno et al., 2000), was investigated with ^{125}I-MT7ox. Staurosporine completely inhibits ^{125}I-MT7ox binding, with a pK_x equal to 6.29 $\pm$ 0.11, in the same range as that obtained previously from equilibrium binding with [^{3}H]NMS and ACh (pK_x = 5.91 $\pm$ 0.03) (Lazareno et al., 2000). On the other hand, KT5720 shows a positive cooperativity with ^{125}I-MT7ox (Fig. 8A), as was also determined for [^{3}H]NMS and ACh (Lazareno et al., 2000). Given the specific capacity of KT5720 to interact with a second allosteric site on hM1 receptor, distinct from the gallamine or brucine "classic" allosteric site (Lazareno et al., 2000), we can postulate that MT7 interacts with a specific allosteric site on the receptor and its binding can be allosterically modulated either by orthosteric ligands or by allosteric agents interacting with the M_1 receptor. Moreover, the possible simultaneous binding and cooperative interaction between two allosteric ligands on the muscarinic receptor has been reported most recently on the M_2 receptor subtype (Trankle et al., 2005). Furthermore, the toxin allosteric site on the receptor may partially overlap the different allosteric sites identified previously for small ligands, as suggested by the common functional role of the extracellular loop e2 of muscarinic receptors in the interaction of MT7 (Kukkonen et al., 2004) and typical or "atypical" allosteric ligands (Leppik et al., 1994; Gnagey et al., 1999; Krejci and Tucek, 2001; Voigtlander et al., 2003; Trankle et al., 2005).

Two orthosteric ligands, NMS and atropine, did not fully inhibit the binding of ^{125}I-MT7ox to the free hM_1 receptor (Fig. 8A), which provides estimates of their affinity for this receptor and highlights their strong negative cooperativity with the toxin (Table 2). According to the ternary complex model, the calculated affinities (pK_x) are in good agreement with the subnanomolar pK_i constants measured in competition experiments with [^{3}H] NMS (Table 2).

Binding experiments with MT1 toxin were performed with both radiotracers. The mode of interaction of this muscarinic toxin with hM_1 receptor is not completely clear but seems to differ from that of MT7 toxin. For example, unlike MT7, MT1 does not affect the [^{3}H]NMS dissociation and interacts reversibly with hM_1 receptor (Mourier et al., 2003). It is clear that MT1 does not affect the ^{125}I-MT7ox dissociation kinetics (Fig. 7 and Table 1) and completely inhibits specific ^{125}I-MT7 binding to unliganded hM_1 receptor with a slope factor not significantly different from unity (Fig. 8B, Table 2). Thus, even if we cannot exclude definitively an allosteric interaction of MT1 with a high negative cooperativity with ^{125}I-MT7ox, the two toxins seem to interact competitively on hM_1 receptor. Nevertheless, they induce different effects on [^{3}H]NMS binding and possess various functional properties as reported in the literature: allosteric modulator for MT7 (Max et al., 1993; Olianas et al., 2000, 2004; Krajewski et al., 2001; Mourier et al., 2003) and agonist for MT1 (Jerusalinsky et al., 1993; Harvey et al., 2002). The molecular origin of the specific pharmacological profiles of these two toxins on hM_1 receptor is still unknown and can now be examined with two different radiotracers.

In conclusion, MT7 toxin, the most potent and specific allosteric modulator on M_1 receptor, was iodinated and used as radiotracer to characterize the interaction of various ligands with the free state of this receptor, thus opening up new perspectives in the study of the interaction of toxins and allosteric agents on M_1 muscarinic receptors. Comparison of the effects of these agents on both ^{125}I-MT7ox and [^{3}H]NMS binding suggests that MT7 interacts at a specific allosteric site on the receptor and that its interaction can be allosterically modulated by orthosteric or allosteric compounds. In addition, various derivatives of the iodinated toxins could be used to specifically label, reversibly or irreversibly, the M_1 receptor in vivo to improve our knowledge of the precise location of this receptor subtype. Finally, changes in the toxin's affinity as a result of the modification of its sequence should be studied directly using ^{125}I-MT7ox and compared with preliminary results obtained indirectly with [^{3}H]NMS as tracer. Thus, the functional site by which MT7 interacts with free and NMS-occupied M_1 receptor will be clearly delineated.

Acknowledgments

We thank Professors P. O. Couraud and A. D. Strosberg (Institut Cochin de Génétique Moléculaire, Paris, France) for the gift of CHO cells expressing M_1 muscarinic receptors, N. Gilles for help in the iodination experiments and for valuable criticism, and A. Caruana for technical assistance. We are also grateful to N. Birdsall for fruitful discussion.

References

Birdsall NJ, Farries T, Gharagozloo P, Kobayashi S, Kuonen D, Lazareno S, Popham A, and Sugimoto M (1997) Selective allosteric enhancement of the binding and actions of acetylcholine at muscarinic receptor subtypes. *Life Sci* **60:**1047–1052.

Birdsall NJ and Lazareno S (2005) Allosterism at muscarinic receptors: ligands and mechanisms. *Mini Rev Med Chem* **5:**523–543.

Birdsall NJ, Lazareno S, Popham A, and Saldanha J (2001) Multiple allosteric sites on muscarinic receptors. *Life Sci* **68:**2517–2524.

Bradley KN (2000) Muscarinic toxins from the green mamba. *Pharmacol Ther* **85:**87–109.

Cheng Y and Prusoff WH (1973) Relationship between the inhibition constant (Ki) and the concentration of inhibitor which causes 50 per cent inhibition (I50) of an enzymatic reaction. *Biochem Pharmacol* **22:**3099–3108.

Christopoulos A and Kenakin T (2002) G protein-coupled receptor allosterism and complexing. *Pharmacol Rev* **54:**323–374.

Christopoulos A, Lanzafame F, and Mitchelson F (1998) Allosteric interactions at muscarinic cholinoceptors. *Clin Exp Pharmacol Physiol* **25:**185–194.

Ehlert FJ (1988) Estimation of the affinities of allosteric ligands using radioligand binding and pharmacological null methods. *Mol Pharmacol* **33:**187–194.

Ellis J (1997) Allosteric binding sites on muscarinic receptors. *Drug Dev Res* **40:**193–204.

Ellis J, Seidenberg M, and Brann MR (1993) Use of chimeric muscarinic receptors to investigate epitopes involved in allosteric interactions. *Mol Pharmacol* **44:**583–588.

Gnagey AL, Seidenberg M, and Ellis J (1999) Site-directed mutagenesis reveals two epitopes involved in the subtype selectivity of the allosteric interactions of gallamine at muscarinic acetylcholine receptors. *Mol Pharmacol* **56:**1245–1253.

Harvey AL, Kornisiuk E, Bradley KN, Cervenansky C, Duran R, Adrover M, Sanchez G, and Jerusalinsky D (2002) Effects of muscarinic toxins MT1 and MT2 from green mamba on different muscarinic cholinoceptors. *Neurochem Res* **27:**1543–1554.

Jerusalinsky D, Cervenansky C, Walz R, Bianchin M, and Izquierdo I (1993) A peptide muscarinic toxin from the Green Mamba venom shows agonist-like action in an inhibitory avoidance learning task. *Eur J Pharmacol* **240:**103–105.

Karlsson E, Jolkonen M, Mulugeta E, Onali P, and Adem A (2000) Snake toxins with high selectivity for subtypes of muscarinic acetylcholine receptors. *Biochimie* **82:**793–806.

Krajewski JL, Dickerson IM, and Potter LT (2001) Site-directed mutagenesis of m1-toxin1: two amino acids responsible for stable toxin binding to M_1 muscarinic receptors. *Mol Pharmacol* **60:**725–731.

Krejci A and Tucek S (2001) Changes of cooperativity between N-methylscopolamine and allosteric modulators alcuronium and gallamine induced by mutations of external loops of muscarinic M_3 receptors. *Mol Pharmacol* **60:**761–767.

Kukkonen A, Perakyla M, Akerman KE, and Nasman J (2004) Muscarinic toxin 7 selectivity is dictated by extracellular receptor loops. *J Biol Chem* **279:**50923–50929.

Lazareno S and Birdsall NJ (1995) Detection, quantitation and verification of allosteric interactions of agents with labeled and unlabeled ligands at G protein-coupled receptors: interactions of strychnine and acetylcholine at muscarinic receptors. *Mol Pharmacol* **48:**362–378.

Lazareno S, Dolezal V, Popham A, and Birdsall NJ (2004) Thiochrome enhances acetylcholine affinity at muscarinic M4 receptors: receptor subtype selectivity via cooperativity rather than affinity. *Mol Pharmacol* **65:**257–266.

Lazareno S, Gharagozloo P, Kuonen D, Popham A, and Birdsall NJ (1998) Subtype-selective positive cooperative interactions between brucine analogues and acetylcholine at muscarinic receptors: radioligand binding studies. *Mol Pharmacol* **53:**573–589.

Lazareno S, Popham A, and Birdsall NJ (2000) Allosteric interactions of staurosporine and other indolocarbazoles with *N*-[methyl-^{3}H]scopolamine and acetylcholine at muscarinic receptor subtypes: identification of a second allosteric site. *Mol Pharmacol* **58:**194–207.

Lazareno S, Popham A, and Birdsall NJ (2002) Analogs of WIN 62,577 define a second allosteric site on muscarinic receptors. *Mol Pharmacol* **62:**1492–1505.

Lee NH and el-Fakahany EE (1991) Allosteric interactions at the m1, m2 and m3 muscarinic receptor subtypes. *J Pharmacol Exp Ther* **256:**468–479.

Leppik RA, Miller RC, Eck M, and Paquet JL (1994) Role of acidic amino acids in the allosteric modulation by gallamine of antagonist binding at the m2 muscarinic acetylcholine receptor. *Mol Pharmacol* **45:**983–990.

Lu ZL, Saldanha JW, and Hulme EC (2001) Transmembrane domains 4 and 7 of the M_1 muscarinic acetylcholine receptor are critical for ligand binding and the receptor activation switch. *J Biol Chem* **276:**34098–34104.

Matsui H, Lazareno S, and Birdsall NJ (1995) Probing of the location of the allosteric site on m1 muscarinic receptors by site-directed mutagenesis. *Mol Pharmacol* **47:**88–98.

Max SI, Liang JS, and Potter LT (1993) Stable allosteric binding of m1-toxin to m1 muscarinic receptors. *Mol Pharmacol* **44:**1171–1175.

May LT and Christopoulos A (2003) Allosteric modulators of G-protein-coupled receptors. *Curr Opin Pharmacol* **3:**551–556.

Mourier G, Dutertre S, Fruchart-Gaillard C, Ménez A, and Servent D (2003) Chemical synthesis of MT1 and MT7 muscarinic toxins: critical role of Arg-34 in their interaction with M1 muscarinic receptor. *Mol Pharmacol* **63:**26–35.

Mourier G, Servent D, Zinn-Justin S, and Ménez A (2000) *Chemical* engineering of a three-fingered toxin with anti-α7 neuronal acetylcholine receptor activity. *Protein Eng* **13:**217–225.

Olianas MC, Adem A, Karlsson E, and Onali P (2004) Action of the muscarinic toxin MT7 on agonist-bound muscarinic M1 receptors. *Eur J Pharmacol* **487:**65–72.

Olianas MC, Maullu C, Adem A, Mulugeta E, Karlsson E, and Onali P (2000) Inhibition of acetylcholine muscarinic M_1 receptor function by the M_1-selective ligand muscarinic toxin 7 (MT-7). *Br J Pharmacol* **131:**447–452.

Onali P, Adem A, Karlsson E, and Olianas MC (2005) The pharmacological action of MT-7. *Life Sci* **76:**1547–1552.

Potter LT, Ferrendelli CA, Hanchett HE, Hollifield MA, and Lorenzi MV (1989) Tetrahydroaminoacridine and other allosteric antagonists of hippocampal M1 muscarine receptors. *Mol Pharmacol* **35:**652–660.

Rusconi L and Montecucchi PC (1985) Reversed-phase high performance liquid chromatography of natural and synthetic sauvagines. *Chromatography* **346:**390–395.

Stockton JM, Birdsall NJ, Burgen AS, and Hulme EC (1983) Modification of the binding properties of muscarinic receptors by gallamine. *Mol Pharmacol* **23:**551–557.

Trankle C, Dittmann A, Schulz U, Weyand O, Buller S, Johren K, Heller E, Birdsall NJ, Holzgrabe U, Ellis J, et al. (2005) Atypical muscarinic allosteric modulation: cooperativity between modulators and their atypical binding topology in muscarinic M2 and M2/M5 chimeric receptors. *Mol Pharmacol* **68:**1597–1610.

Trankle C, Mies-Klomfass E, Cid MH, Holzgrabe U, and Mohr K (1998) Identification of a [3H]ligand for the common allosteric site of muscarinic acetylcholine M2 receptors. *Mol Pharmacol* **54:**139–145.

Trankle C and Mohr K (1997) Divergent modes of action among cationic allosteric modulators of muscarinic M2 receptors. *Mol Pharmacol* **51:**674–682.

Trankle C, Weyand O, Schroter A, and Mohr K (1999) Using a radioalloster to test predictions of the cooperativity model for gallamine binding to the allosteric site of muscarinic acetylcholine M_2 receptors. *Mol Pharmacol* **56:**962–965.

Trankle C, Weyand O, Voigtlander U, Birdsall NJ, Mohr K, Mynett A, and Lazareno S (2003) Interactions of orthosteric and allosteric ligands with [^{3}H]dimethyl-W84 at the common allosteric site of muscarinic M2 receptors. *Mol Pharmacol* **64:**180–190.

Tucek S and Proska J (1995) Allosteric modulation of muscarinic acetylcholine receptors. *Trends Pharmacol Sci* **16:**205–212.

Voigtlander U, Johren K, Mohr M, Raasch A, Trankle C, Buller S, Ellis J, Holtje HD, and Mohr K (2003) Allosteric site on muscarinic acetylcholine receptors: identification of two amino acids in the muscarinic m2 receptor that account entirely for the m2/m5 subtype selectivities of some structurally diverse allosteric ligands in *N*-methylscopolamine-occupied receptors. *Mol Pharmacol* **64:**21–31.

Address correspondence to: Dr. D. Servent, CEA, Département d'Ingénierie et d'Etude des Protéines, 91191 Gif-sur-Yvette, France. E-mail: denis.servent@cea.fr